Electronic Supporting Information for:

A H-aggregating fluorescent probe for recognizing both mercury and copper ions based on a dicarboxyl-pyridyl bifunctionalized difluoroboron dipyrromethene

Hao-Ran Xie†, Ya-Qi Gu†, Li Liu and Jing-Cao Dai*

Institute of Materials Physical Chemistry, Huaqiao University, Xiamen, Fujian 361021, China

† Contributed equally.

* Corresponding author, Email: djc@hqu.edu.cn.

Content

TableS1. Crystal Data Collections and Structure Refinement Parameters for 2,6-diCO_2Bzl-BODIPY

Compound	2,6-diCO_2Bzl-BODIPY
CCDC code	1484737
empirical formula	$C_{34}H_{30}BF_2N_3O_4$
formula weight	593.42
T (°K)	293(2)
λ (Å)	0.71073 (Mo–$K\alpha$)
Crystal system, Space group, Z	Triclinic , $P\bar{1}$, 2
a, b, c (Å)	9.0378(7), 13.014(1),14.511(1)
α, β, γ (°)	114.894(8), 96.065(6), 100.583(7)
V (Å^3)	1489.5(2)
ρ_{calcd} (g·cm^3)	1.323
μ (mm^{-1})	0.095
F(000)	620
Crystal size (mm)	0.50×0.20×0.16
θ Range (°)	2.8 – 25.0
Collected reflections	9721
Unique reflections	5121
Observed reflections	2432
R_{int}	0.0629
Data / restraints / parameters	5121 / 0 / 398
GOF	1.022
R indices (for obs.):	
R_1 [a], wR_2 [b]	0.0707, 0.1625
R indices (for all):	
R_1, wR_2	0.1592, 0.2124
Largest diff. peak/hole (e.Å^{-3})	0.29/-0.22

[a] $R_1 = \sum(||F_o|-|F_c||)/\sum|F_o|$, $wR_2 = \{\sum w[(F_o^2-F_c^2)^2]/\sum w[(F_o^2)^2]\}^{1/2}$; [b] $w = 1/[\sigma^2(F_o^2)+(aP)^2+bP]$, where $P = (F_o^2+2F_c^2)/3$].

Table S2. Geometrical Parameters for 2,6-diCO_2Bzl-BODIPY [Å and °].

Selected bond lengths and angles			
Bond lengths		Bond angles	
B-F(1)	1.376(5)	F(1)-B-F(2)	109.2(4)
B-F(2)	1.371(5)	F(1)-B-N(2)	110.2(3)
B-N(2)	1.535(5)	F(1)-B-N(3)	110.1(4)
B-N(3)	1.540(5)	F(2)-B-N(2)	110.4(4)
N(1)-C(16)	1.330(6)	F(2)-B-N(3)	109.7(3)
N(1)-C(20)	1.310(6)	N(2)-B-N(3)	107.2(3)
N(2)-C(5)	1.344(5)	B-N(2)-C(5)	125.4(3)
N(2)-C(9)	1.398(4)	B-N(2)-C(9)	125.9(3)
N(3)-C(3)	1.339(5)	B-N(3)-C(3)	125.8(3)
N(3)-C(4)	1.395(4)	B-N(3)-C(4)	125.5(3)
O(1)-C(10)	1.196(5)		
O(2)-C(10)	1.309(5)		
O(3)-C(11)	1.203(5)		
O(4)-C(11)	1.323(5)		
Hydrogen bonds				
D-H...A	d(D-H)	d(H...A)	d(D...A)	<(DHA)
C(13)-H(13A)...O(2)	0.96	2.25	2.912(6)	125.6
C(13)-H(13B)...F(2)	0.96	2.58	3.089(5)	113.2
C(13)-H(13C)...F(1)	0.96	2.63	3.101(5)	110.4
C(15)-H(15A)...O(3)	0.96	2.30	3.008(6)	129.6
C(15)-H(15B)...F(1)	0.96	2.60	3.067(5)	110.3
C(17)-H(17A)...O(3*a*)	0.93	2.58	3.419(6)	151.0
C(19)-H(19A)...F(1*b*)	0.93	2.51	3.289(5)	141.8
C(34)-H(34B)...O(1*c*)	0.97	2.64	3.495(7)	146.7

Symmetry transformations used to generate equivalent atoms:
a = -x,-y+1,-z; *b* = -x+1,-y+1,-z; *c* = x-1,y-1,z-1

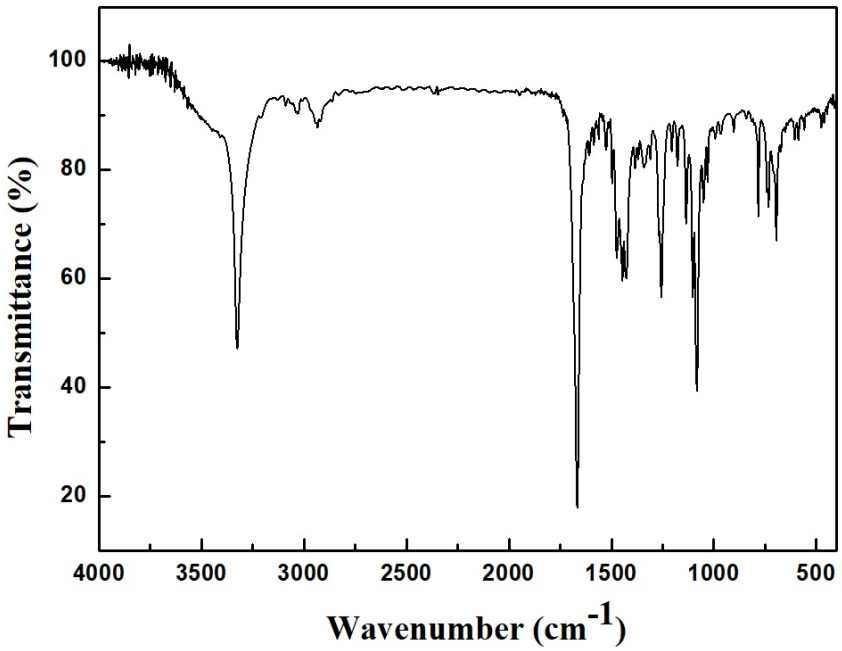

Figure S1 FT-IR spectra of benzyl 2,4-dimethyl-1*H*-pyrrole-3-carboxylate

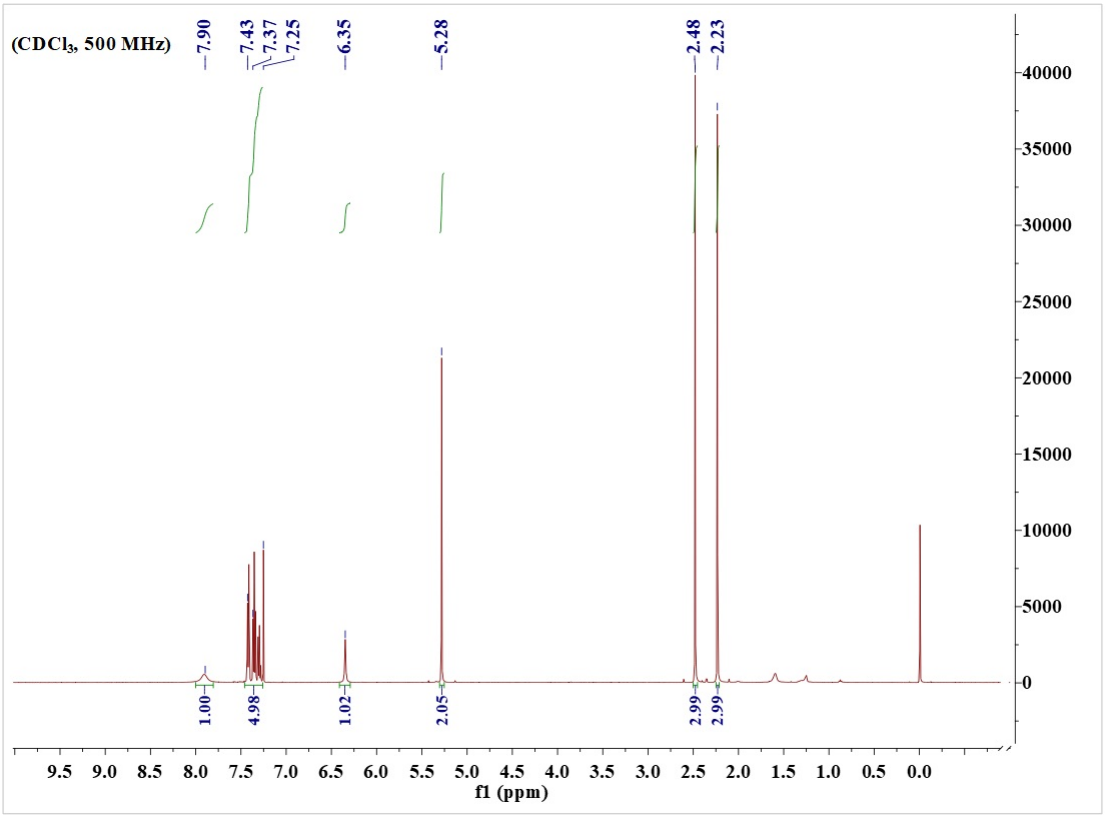

Figure S2 ^{1}H NMR spectra of benzyl 2,4-dimethyl-1*H*-pyrrole-3-carboxylate

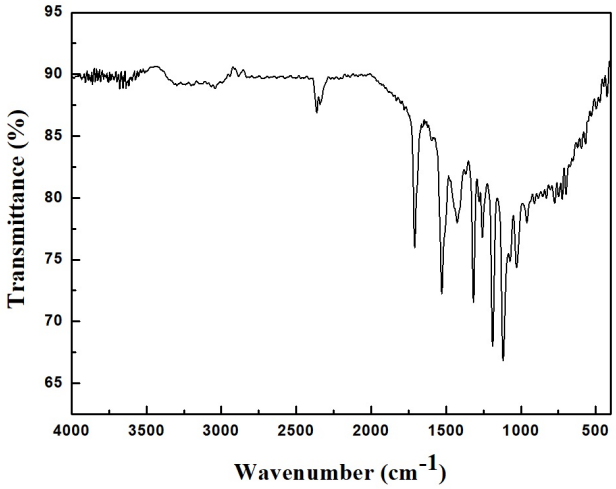

Figure S3 FT-IR spectra of 2,6-diCO_2Bzl-BODIPY

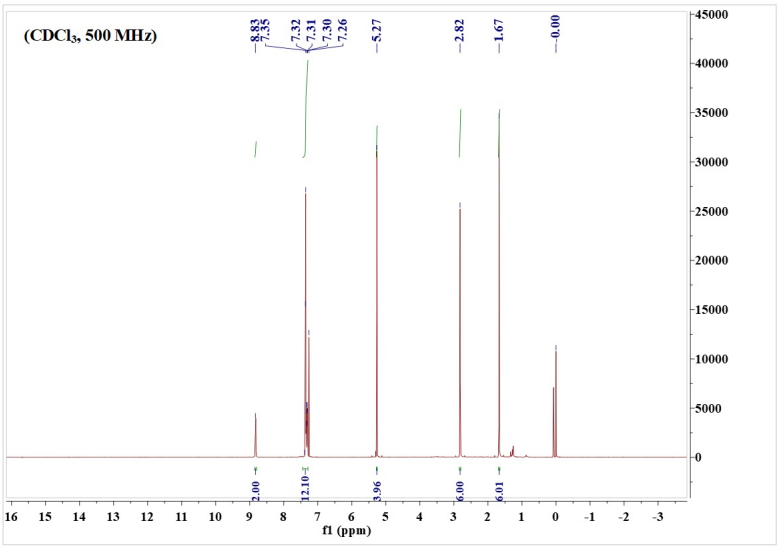

Figure S4 ^{1}H NMR spectra of 2,6-diCO_2Bzl-BODIPY

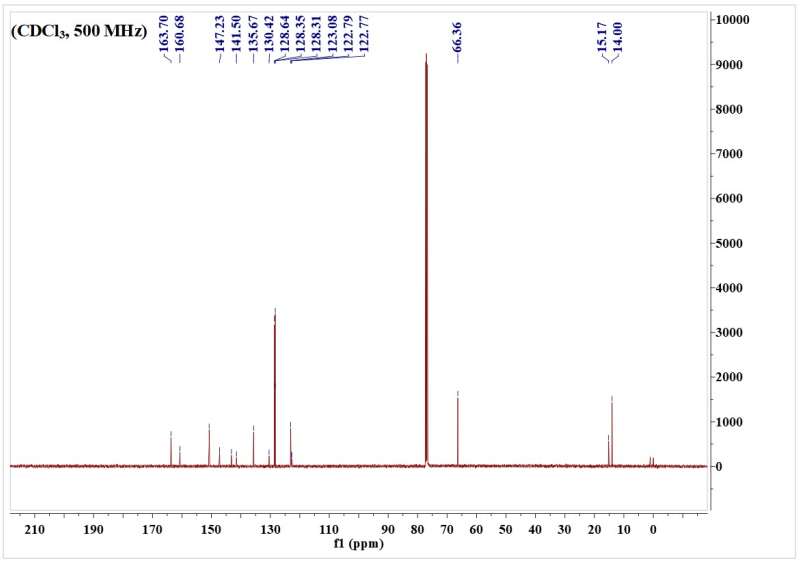

Figure S5 ^{13}C NMR spectra of 2,6-diCO_2Bzl-BODIPY

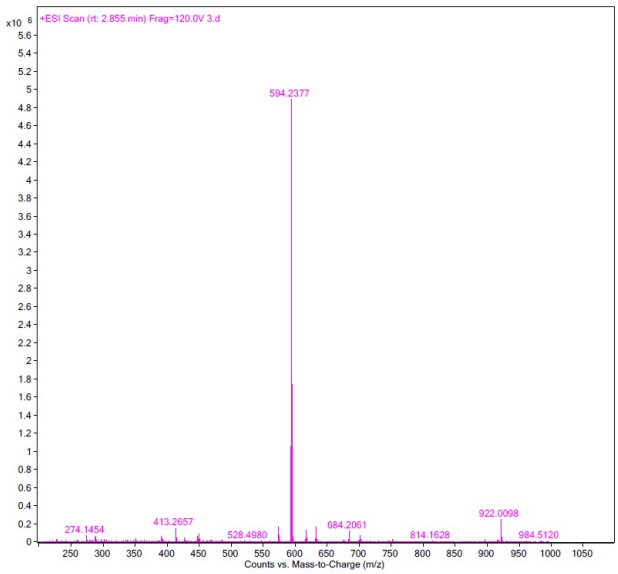

Figure S6 ESI-MS data of 2,6-diCO_2Bzl-BODIPY

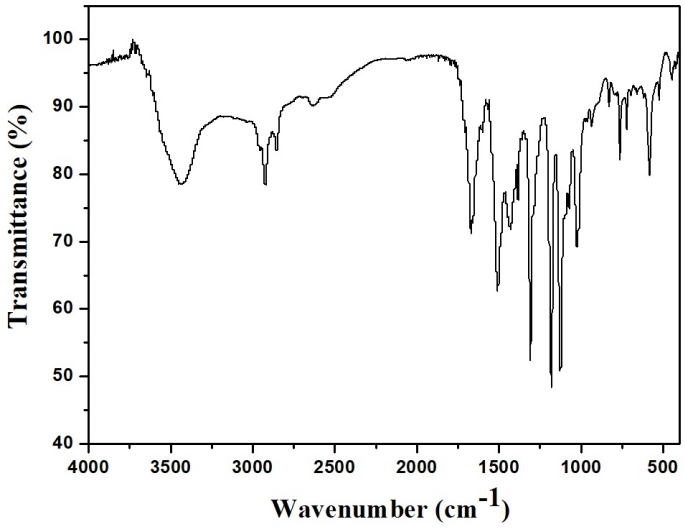

Figure S7 FT-IR spectra of 2,6-diCO_2H-BODIPY

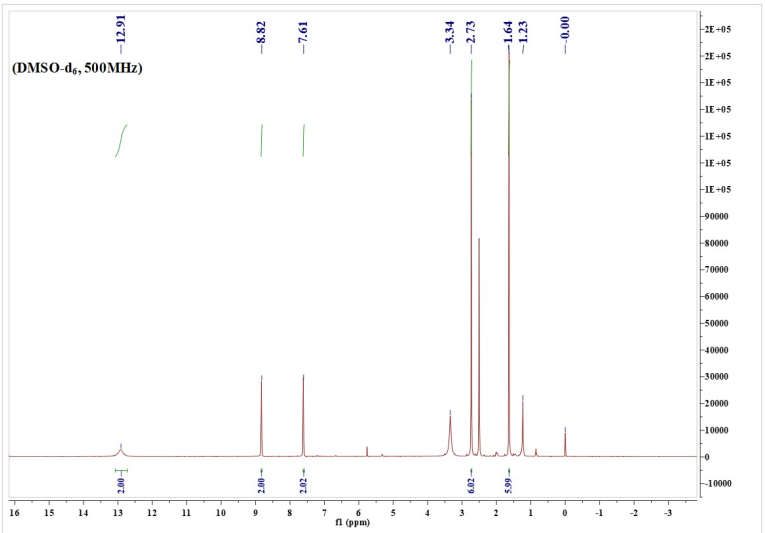

Figure S8 ^{1}H NMR spectra of 2,6-diCO_2H-BODIPY

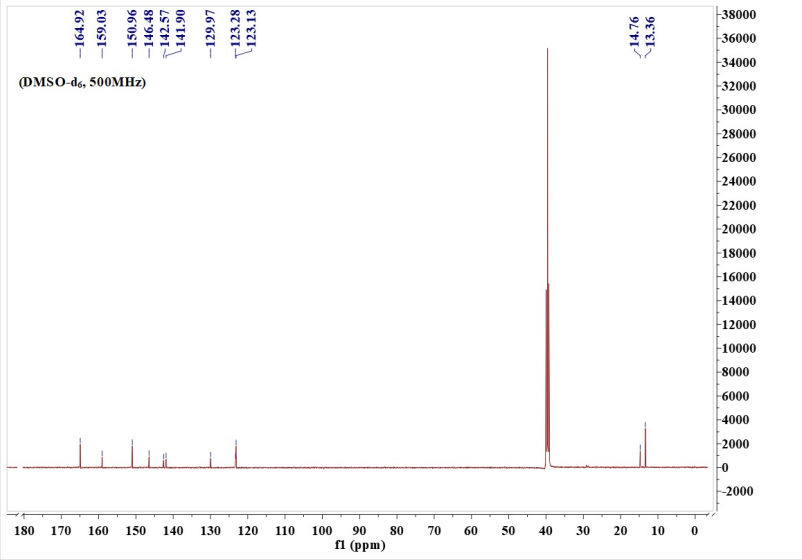

Figure S9 ^{13}C NMR spectra of 2,6-diCO_2H-BODIPY

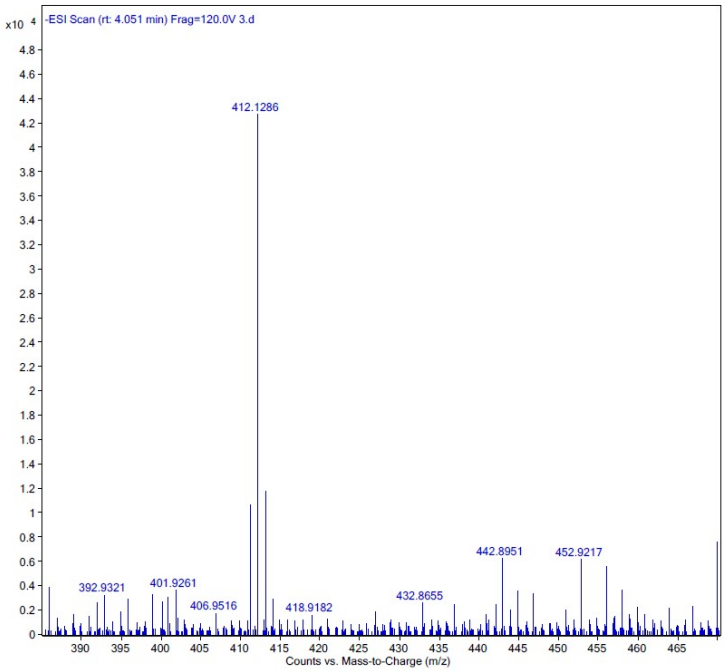

Figure S10 ESI-MS data of 2,6-diCO_2H-BODIPY

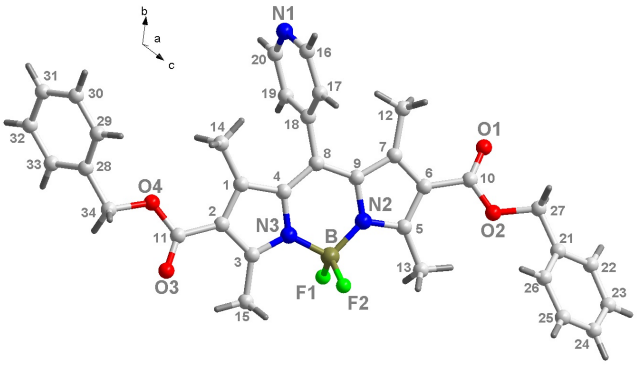

a

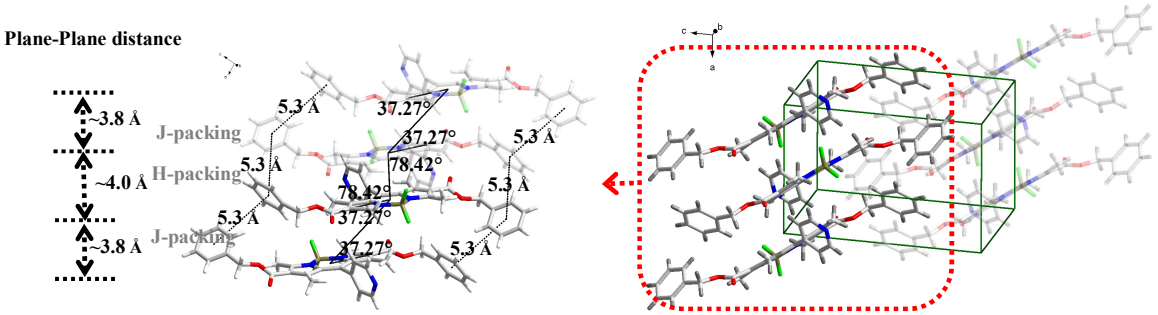

b

Figure S11 (*a*) The ORTEP drawing of 2,6-diCO_2Bzl-BODIPY molecule; (b) A view showing the 2,6-diCO_2Bzl-BODIPY molecules parallel packing in the chain-like supramecular aggregates with an alternating head-to-tail orientation in unit cell (righ), in which the alternating H-type to J-type packings (left) are resulted from T-shaped edge-to-face and vertex-to-face C-H…π interactions of phenyl-phenyl embraces.

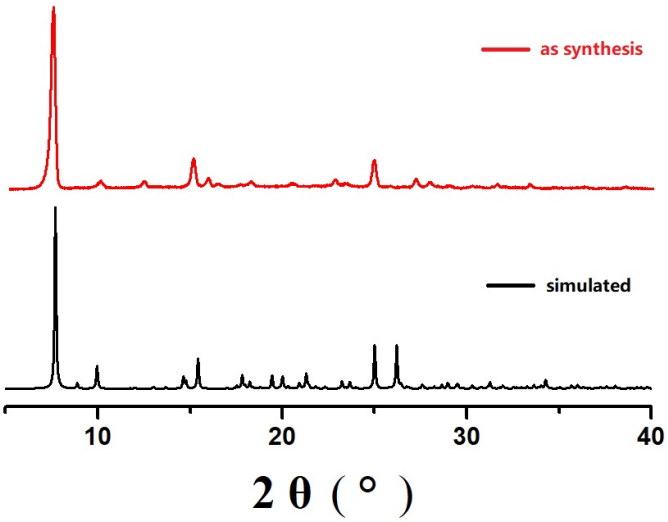

Figure S12 XRD of 2,6-diCO_2H-BODIPY

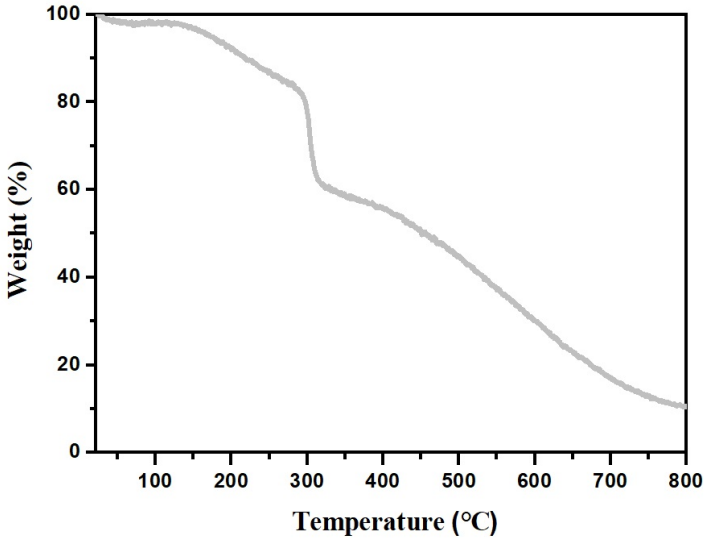

Figure S13 TGA trace of 2,6-diCO_2H-BODIPY

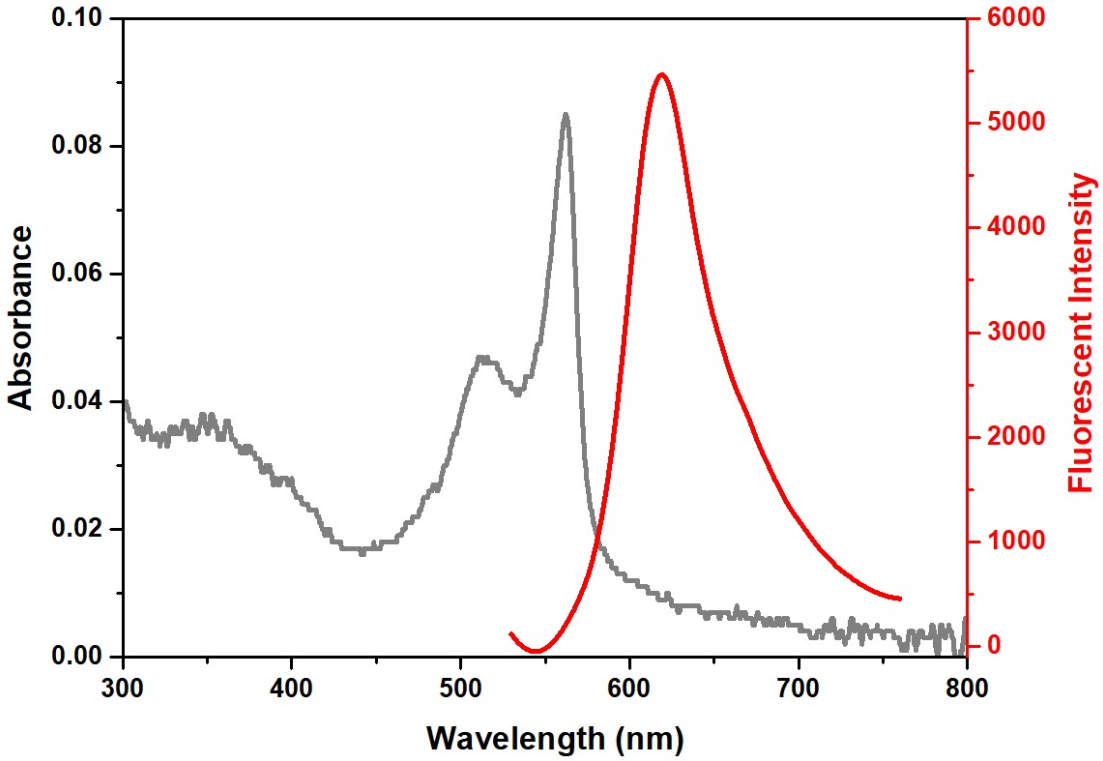

Figure S14 The solid-state absorbance (gray) and emission (red) spectra of 2,6-diCO_2H-BODIPY

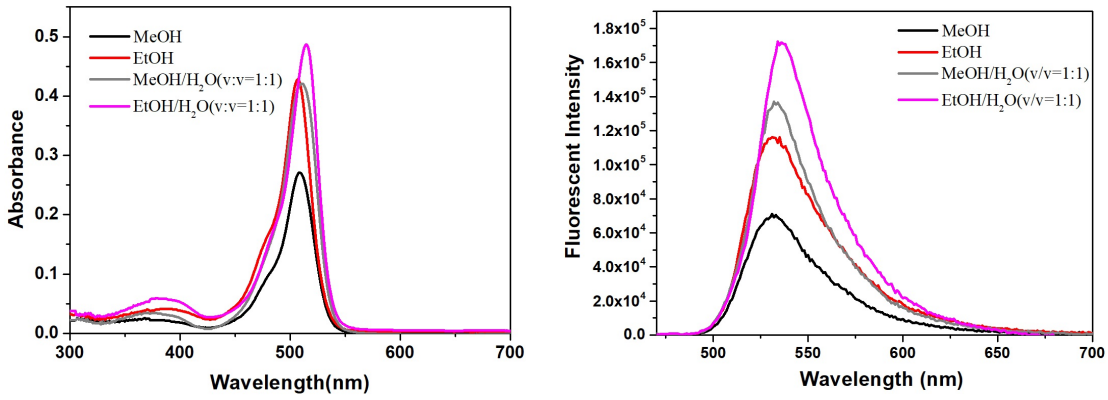

(*a*) (*b*)

Figure S15 (*a*) The absorbance and (*b*) emission (λ_{ex} = 360 nm) spectra of a 10 μM solution of 2,6-diCO_2H-BODIPY in four different solvents.

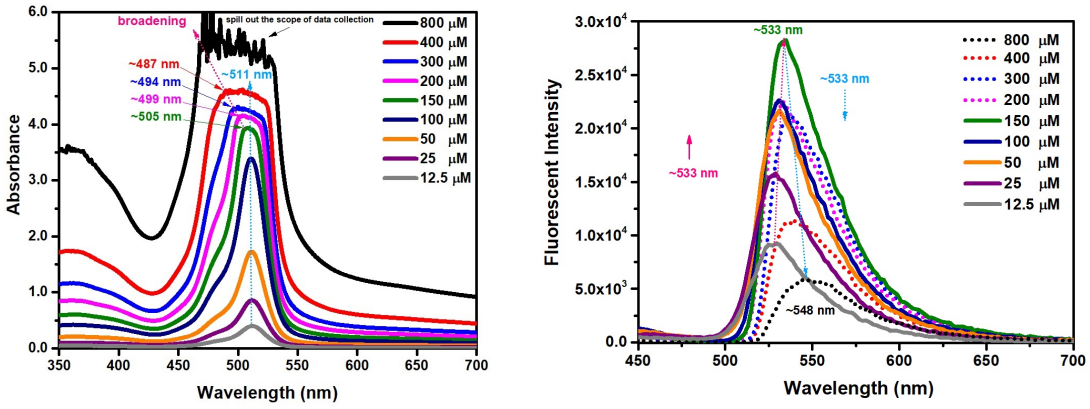

(*a*) (*b*)

Figure S16 (*a*) The absorbance and (*b*) emission (λ_{ex} = 360 nm) spectra of 2,6-diCO_2H-BODIPY at different concentrations in v/v=1:1 MeOH/H_2O solution.

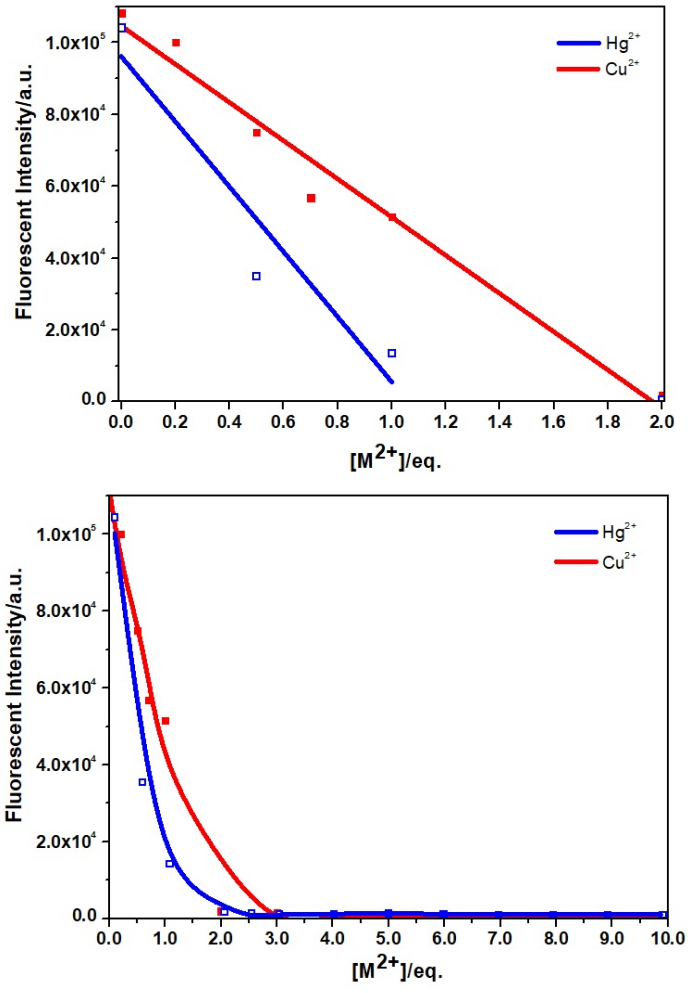

Figure S17 Job's plot of the relationship between fluorescent intensity of 2,6-diCO_2H-BODIPY probe and the addition of metal ions ranging from 0 to 2.0 eq. (top) and 0 to 10 eq. (bottom)

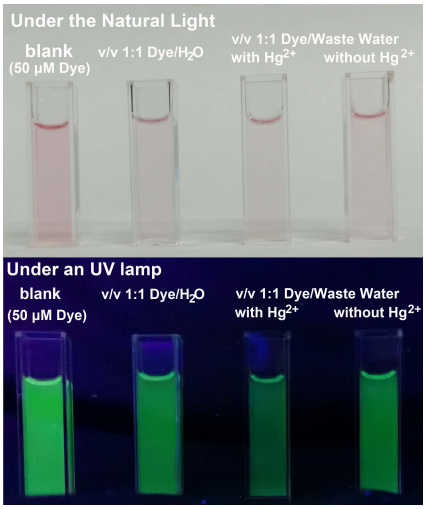

Figure S18 The photos showing the naked eye visible fluorescent color changes in a 50 μM 2,6-diCO_2H-BODIPY in v/v=1:1 MeOH/H_2O solution upon addition of isochoric distilled water, the mercury-containing subacidic wastewater (pH = ~6.2) from battery factory (metal ion pollutant: ~14 mg·L^{-1} Hg^{2+}, ~194 mg·L^{-1} Zn^{2+}, ~28 mg·L^{-1} Mn^{2+}), and the same subacidic wastewater (pH = ~6.2) from battery factory but after treatment of mercury removal (metal ion pollutant: <<~0.5 μg·L^{-1} Hg^{2+}, ~146 mg·L^{-1} Zn^{2+}, ~25 mg·L^{-1} Mn^{2+}) after exposure on the natural light (upper) and an UV lamp (bottom, 365 nm).

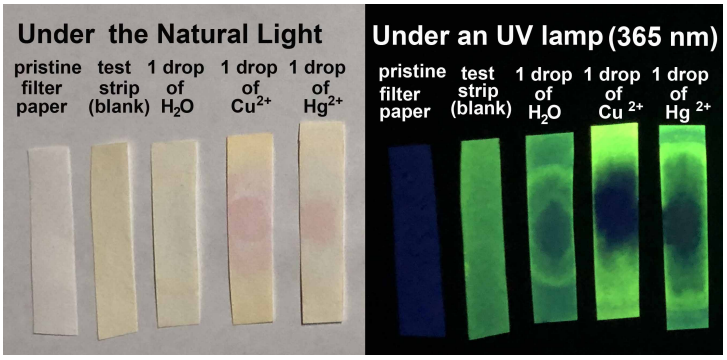

Figure S19 The photos of paper-based test strip containing ~0.03 Mg·cm^{-2} of 2,6-diCO_2H-BODIPY, which fabricated by ~1.0×5.0 cm filter paper dipping in a 50 μM 2,6-diCO_2H-BODIPY in v/v=1:1 MeOH/H_2O solution, showing the naked eye visible color changes after exposure by 1 drop of 10 eq. of either copper or mercury ion under the natural light (left) and an UV lamp (right, 365 nm).

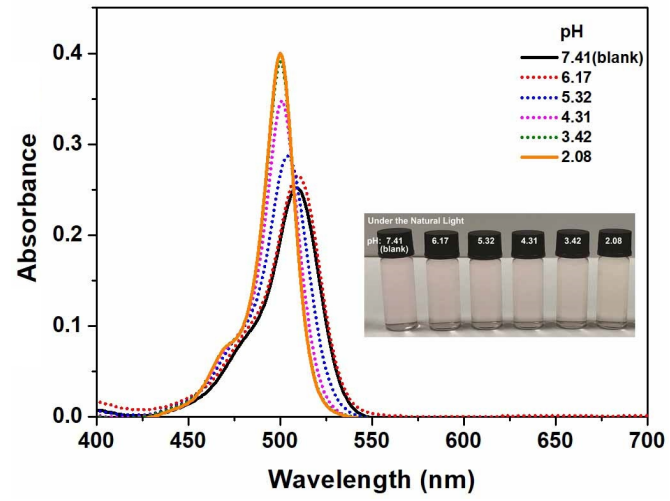

(*a*)

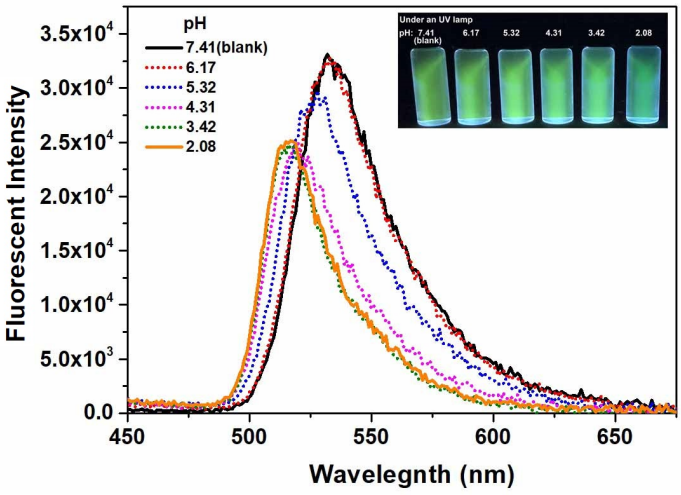

(*b*)

Figure S20 (*a*) The absorbance and (*b*) emission (λ_{ex} = 360 nm) spectra of 2,6-diCO_2H-BODIPY (10 μM in v/v=1:1 MeOH/H_2O solution) in a pH range of 2.8-7.41. Inset shows photographs of each pH value under the natural light (upper) or an UV lamp (bottom, 365 nm).